Electrochim. Acta

Dye Sensitization of Polymer/Fullerene Solar Cells Incorporating Bulky Phthalocyanines

Huajun XU[1], Takaaki WADA[1,*], Hideo OHKITA[1,2,a)], Hiroaki BENTEN[1], Shinzaburo ITO[1]

[1]*Department of Polymer Chemistry, Graduate School of Engineering, Kyoto University, Katsura, Nishikyo, Kyoto 615-8510, Japan*

[2]*Japan Science and Technology Agency (JST), PRESTO, 4-1-8 Honcho Kawaguchi, Saitama 332-0012, Japan*

a) Author to whom correspondence should be addressed; FAX: +81-75-383-2617; electronic mail: ohkita@photo.polym.kyoto-u.ac.jp

Abstract

The light-harvesting efficiency of P3HT:PCBM solar cells can be improved by incorporating near-IR dye molecules such as silicon phthalocyanine derivatives with bulky axial groups (SiPc). In order to study the size effect of the axial groups on the dye sensitization in P3HT:PCBM solar cells, we synthesized five SiPc derivatives with different axial groups: SiPc[OSi(C_nH_{2n+1})$_3$]$_2$ (SiPc*n*, *n* = 2, 3, 4, 6) and SiPc[OSi(iBu)$_2$$C_{18}H_{37}$]$_2$ (SiPcB18). The power conversion efficiency (PCE) increased in the order of *n* = 2 to 4, reached the maximum at around *n* = 4 and 6, and then decreased for SiPcB18 with the longest axial groups. As a result, the PCE was improved to 4.2%, which is larger by 10% than that of P3HT:PCBM control cells without dye molecules. We therefore conclude that the butyl or hexyl chain in the axial ligand is the most appropriate for the dye sensitization in P3HT:PCBM solar cells.

Keywords

Dye sensitization; Silicon phthalocyanine; Polymer solar cell; Axial ligand; Aggregation

1. Introduction

Polymer solar cells based on a blend of a conjugated polymer and a fullerene derivative have attracted interest because of their potential to be lightweight, flexible, solution processable, and hence cost-effective.[1–5] Among them, the blend of regioregular poly(3-hexylthiophene) (P3HT) and [6,6]-phenyl-C_{61}-butyric acid methyl ester (PCBM) has been most widely studied as the active layer in polymer/fullerene solar cells. This polymer solar cell exhibits high external quantum efficiency (EQE) and fill factor (FF),[6–10] which are still the highest in polymer solar cells. However, P3HT can harvest only up to ~650 nm, which corresponds to only a quarter of the total photons in the solar light. In order to harvest a broader range of the solar light, various low-bandgap polymers have been developed in recent years.[11–14] On the other hand, dye sensitization based on a ternary blend of polymer/fullerene/dye has been recently reported as another approach to expand the light-harvesting range by several groups including ours.[15–19]

We have shown that the light-harvesting efficiency of P3HT:PCBM solar cells can be improved by incorporating silicon phthalocyanine bis(trihexylsilyl oxide) (SiPc6).[16] Furthermore, we demonstrated that the light-harvesting bandwidth can be expanded by multi-colored sensitization with SiPc6 and silicon naphthalocyanine bis(trihexylsilyl oxide) (SiNc6), which have complementary absorption bands in the near-IR region.[17] The bulky trihexylsilyl oxide group can effectively suppress dye aggregation even in solid films and therefore is considered to be one of the keys to success. However, such bulky substituents could hinder the charge transfer between the neighboring molecules. In other words, little is known about the appropriate size of substituents for dye-sensitized polymer/fullerene solar cells.

In this study, we synthesized a series of SiPc derivatives with the same two trialkylsilyl oxide axial groups -OSi(C_nH_{2n+1})$_3$ to study the size effect of bulky axial groups on the dye sensitization in polymer/fullerene solar cells. The alkyl chains of the two axial

groups systematically vary from ethyl to hexyl in SiPc[OSi(C_nH_{2n+1})$_3$]$_2$ (SiPc*n*, *n* = 2, 3, 4, 6) and the longest of octadecyl in SiPc[OSi(iBu)$_2$$C_{18}H_{37}$]$_2$ (SiPcB18). Herein we discuss the device performance of P3HT:PCBM:dye ternary blend solar cells in terms of steric structures of dye molecules.

2. Experimental

2.1. Synthesis of dye derivatives

Figure 1 shows the reaction schemes and the chemical structures of SiPc derivatives with various axial groups employed in this study. The axial substituents are summarized in Table 1. Details of the synthesis are described below.

-----<<< Fig. 1 & Table 1 >>>-----

SiPc[OSi(C_2H_5)$_3$]$_2$ (SiPc2): A mixture of SiPc(OH)$_2$ (72.4 mg), chlorotriethylsilane (200 μL), and dry pyridine (10 mL) was refluxed for 5 h. After the solution obtained cooled, the solvent was evaporated and chloroform was added to the residue. The solution was washed with saturated NaCl solution, and then dried over $MgSO_4$. After evaporation of the solvent, the residue was purified by silica gel column chromatography (toluene/hexane = 3/1 (v/v) as eluent) to afford SiPc2 (21.4 mg) as a blue solid (yield = 21%).

TLC (toluene/hexane = 3/1 (v/v)): R_f = 0.85

^{1}H NMR (400 MHz, $CDC1_3$): δ = 9.65 (m, 3,6-Pc, 8H), 8.33 (m, 4,5-Pc, 8H), −1.24 (t, CH_3, 18H), −2.44 (m, α-CH_2, 12H)

UV/Vis ($CHCl_3$): λ_{max} = 669 nm ($\varepsilon = 2.6 \times 10^5\ M^{-1}\ cm^{-1}$)

SiPc[OSi(C_3H_7)$_3$]$_2$ (SiPc3): A mixture of SiPc(OH)$_2$ (75.0 mg), chlorotripropylsilane (180 μL), and dry pyridine (10 mL) was refluxed for 5 h. After the solution obtained cooled, the solvent was evaporated and the residue was washed with pentane. After evaporation of the solvent, the residue was purified by silica gel column chromatography (toluene/hexane = 2/1 (v/v) as eluent) to afford SiPc3 (44.0 mg) as a blue solid (yield = 38%).

TLC (toluene/hexane = 2/1 (v/v)): R_f = 0.92

^{1}H NMR (400 MHz, $CDC1_3$): δ = 9.65 (m, 3,6-Pc, 8H), 8.34 (m, 4,5-Pc, 8H), −0.31 (t, CH_3,

18H), −1.17 (m, β-CH_2, 12H), −2.43 (m, α-CH_2, 12H)

UV/Vis ($CHCl_3$): λ_{max} = 668 nm ($\varepsilon = 3.0 \times 10^5\ M^{-1}\ cm^{-1}$)

SiPc[OSi(C_4H_9)$_3$]$_2$ (SiPc4): A mixture of SiPc(OH)$_2$ (75.4 mg), chlorotributylsilane (210 μL), and dry pyridine (10 mL) was refluxed for 5 h. After the solution obtained cooled, the solvent was evaporated and the residue was washed with pentane. After evaporation of the solvent, the residue was purified by silica gel column chromatography (toluene/hexane = 1/1 (v/v) as eluent) to afford SiPc4 (81.2 mg) as a blue solid (yield = 70%).

TLC (toluene/hexane = 1/1 (v/v)): R_f = 0.90

^{1}H NMR (400 MHz, $CDC1_3$): δ = 9.64 (m, 3,6-Pc, 8H), 8.33 (m, 4,5-Pc, 8H), 0.05 (m, γ-CH_2, CH_3, 30H), −1.26 (m, β-CH_2, 12H), −2.43 (m, α-CH_2, 12H)

UV/Vis ($CHCl_3$): λ_{max} = 668 nm ($\varepsilon = 2.9 \times 10^5\ M^{-1}\ cm^{-1}$)

SiPc[OSi(C_6H_{13})$_3$]$_2$ (SiPc6): A mixture of SiPc(OH)$_2$ (74.7 mg), chlorotrihexylsilane (500 μL), and dry pyridine (10 mL) was refluxed for 5 h. After the solution obtained cooled, the solvent was evaporated and the residue was added chloroform. The solution was washed with saturated NaCl solution, and then dried over $MgSO_4$. After evaporation of the solvent, the residue was purified by silica gel column chromatography (toluene/hexane = 1/2 (v/v) as eluent) to afford SiPc6 (38 mg) as a blue solid (yield = 25%).

TLC (toluene/hexane = 1/2 (v/v)): R_f = 0.87

^{1}H NMR (400 MHz, $CDC1_3$): δ = 9.63 (m, 3,6-Pc, 8H), 8.31 (m, 4,5-Pc, 8H), 0.81 (m, ε-CH_2, 12H), 0.71 (t, CH_3, 18H), 0.36 (m, δ-CH_2, 12H), 0.02 (m, γ-CH_2, 12H), −1.28 (m, β-CH_2, 12H), −2.45 (m, α-CH_2, 12H)

UV/Vis ($CHCl_3$): λ_{max} = 668 nm ($\varepsilon = 3.0 \times 10^5\ M^{-1}\ cm^{-1}$)

SiPc[OSi(iBu)$_2$$C_{18}H_{37}$]$_2$ (SiPcB18): A mixture of SiPc(OH)$_2$ (99.5 mg),

chlorodiisobutyloctadecylsilane (520 μL), and dry pyridine (25 mL) was refluxed for 5 h. After the solution obtained cooled, the solvent was evaporated and the residue was washed with water, and then dried over $MgSO_4$. After evaporation of the solvent, the residue was purified by silica gel column chromatography (toluene/hexane = 1/3 (v/v) as eluent) to afford SiPcB18 (150 mg) as a blue solid (yield = 64%).

TLC (toluene/hexane = 1/3 (v/v)): R_f = 0.90

^{1}H NMR (400 MHz, $CDC1_3$): δ = 9.62 – 9.64 (m, α-Pc, 8H), 8.30 – 8.32 (m, β-Pc, 8H), 1.33 – 0.84 (m, CH_2, 58H), 0.42 (m, δ-$C_{18}H_{35}$, 4H), 0.08 (m, γ-$C_{18}H_{35}$, 4H), −0.55 (m, γ-iBu, 24H), −0.87 (m, β-$C_{18}H_{35}$, 4H), −1.27 (m, β-iBu, 4H), −2.41 – −2.53 (m, α-$C_{18}H_{35}$ and α-iBu, 12H)

UV/Vis ($CHCl_3$): λ_{max} = 670 nm ($\varepsilon = 3.8 \times 10^5\ M^{-1}\ cm^{-1}$)

2.2. Device fabrication

The indium–tin-oxide (ITO) coated glass substrates was cleaned by ultrasonication in toluene, acetone, and ethanol each for 15 min, dried with N_2, and cleaned with a UV–O_3 cleaner for 30 min. A thin layer (~40 nm) of poly(3,4-ethylenedioxythiophene):poly(4-styrenesulfonate) (PEDOT:PSS) (H.C.Starck, PH500) was spin-coated onto the cleaned ITO-coated substrate at 3000 rpm and was baked at 140 °C for 10 min in air. A ternary blend active layer (~200 nm) of P3HT:PCBM:dye was prepared from spin-coating on the PEDOT:PSS-coated ITO substrate at a spin rate of 600 rpm in an N_2-filled glove box. The wet film was slowly dried in a covered petri dish for 60 min in the glove box. The ternary blend solution was prepared as follows: P3HT, PCBM, and dye were dissolved in *o*-dichlorobenzene at a concentration ratio of 20 : 20 : 1.7 mg mL^{-1} ([SiPc] = 4.1 wt%) and then the mixed solution was stirred at 40 °C overnight. An electrode of Ca/Al layer (20/80 nm) was deposited on top of the active layer in sequence at 2.5×10^{-4} Pa. The effective device area was 0.07 cm^2.

2.3. Measurements

Electrochemical properties of dye molecules were examined by cyclic voltammetry. The cyclic voltammograms were measured in a mixed solution of dichlorobenzene and acetonitrile (4:1 v/v) containing 0.1 M tetrabutylammonium hexafluorophosphate perchlorate (Wako, TBAP) with a potentiostat (Perkin–Elmer, 273A). The reference electrode was Ag/AgCl in a saturated KCl aqueous solution and the counter electrode was a Pt wire. The electrolyte solution was deoxygenated by bubbling with N_2 for 30 min before the measurement. Absorption spectra of the blend films were measured with a spectrophotometer (Hitachi, UV-3500). The current density–voltage (*J*–*V*) characteristics of the devices were measured with a DC voltage and current source/monitor (Advantest, R6243) under AM1.5G simulated solar illumination at 100 mW cm^{-2}. The light intensity was corrected with a calibrated silicon photodiode reference cell (Bunkoh-Keiki, BS-520). The EQE spectra were measured with a digital electrometer (Advantest, R8252) under monochromatic light illumination from a 500-W xenon lamp (Thermo Oriel, Model 66921) with optical cut filters and a monochromator (Thermo Oriel, Cornerstone). The illumination was carried out from the ITO side under N_2 atmosphere at room temperature. At least more than 10 devices were fabricated to ensure the reproducibility of the device performance.

2.4. DFT calculation

The molecular geometry and structure of SiPc derivatives were fully optimized using density functional theory (DFT) with the hybrid B3LYP functional and 6-31G basis set.[20–22] Single-point energy calculations were then performed at the B3LYP/6-31G level.

3. Results

3.1. Electrochemical properties

-----<<< Fig. 2 >>>-----

The electrochemical properties of SiPc derivatives were examined by cyclic voltammetry in 0.1 M TBAP dichlorobenzene/acetonitrile solution with ferrocene as an internal reference. Figure 2 shows the cyclic voltammogram of SiPc6 (solid line) and ferrocene (broken line) at a scan rate of 100 mV s^{-1}. The redox peaks at around 1 V are ascribed to the oxidation potential of SiPc6. Assuming that the energy level of the ferrocene/ferrocenium redox couple is 4.8 eV below the vacuum level,[23] the energy level of the highest occupied molecular orbital (HOMO) of SiPc6 is estimated to be 5.4 eV below the vacuum level, which is consistent with the previous report.[24] Table 2 summarizes the HOMO energy levels of all the SiPc derivatives. As shown in the table, the HOMO levels are independent of the substituents, suggesting that the axial groups have little impact on the electronic state of the phthalocyanine unit.

-----<<< Table 2 >>>-----

3.2. Absorption spectra

Figure 3a shows the absorption spectra of SiPc derivatives in toluene solution. All the dye molecules exhibited a sharp absorption band at 670 nm with almost the same molar absorption coefficient. The absorption peak at 670 nm is ascribed to the Q band of the phthalocyanine unit, from which the optical bandgap can be estimated to be 1.9 eV. Thus, the energy level of the lowest unoccupied molecular orbital (LUMO) of the dye molecules is

estimated to be 3.5 eV by subtracting the optical bandgap from the HOMO level. As summarized in Table 2, all the HOMO and LUMO levels are independent of the axial substituents. These results again suggest that the axial groups have little impact on the electronic state in the phthalocyanine unit.

-----<<< Fig. 3 >>>-----

Figure 3b shows the absorption efficiency of P3HT:PCBM:dye ternary blend films, which is estimated from twice the absorbance on the assumption that the incident light loss at the air/glass interface is 4% and the reflection at the metal electrode is 100%.[25] The absorption efficiency around 400 – 600 nm, which is ascribed to P3HT band, was almost 100% independently of dye molecules. On the other hand, the absorption spectra of dye are significantly different between SiPc2 and the others in contrast to those in toluene solution. The absorption efficiency of SiPc2 was as low as ~20%. The absorption band was split into two bands, suggesting the formation of π stacked aggregates in blend films. The absorption efficiency of the other dyes was as high as ~70% even in blend films although the peak wavelength was slightly red-shifted (~5 nm) compared to those in solution. This finding suggests that the propyl chain (SiPc3) in the axial ligand is large enough to effectively suppress the dye aggregation even in solid films. Furthermore, such long axial groups are required on both sides of the phthalocyanine plane to suppress the dye aggregation effectively.

3.3. Molecular structures

To understand the molecular structures of SiPc derivatives, we performed DFT calculation of these molecules. Figure 4 shows the space-filling structures of SiPc2 and SiPc3 obtained by the DFT calculation. In SiPc2, there is still enough space for another SiPc2 molecule to approach to the phthalocyanine plane, because the end methyl groups in

the axial ligand are attached to the methylene group in the direction normal to the plane. In SiPc3, there is limited space for another SiPc3 molecule to approach to the phthalocyanine plane, because the end methyl groups in the axial ligand are attached to the ethylene group in the direction rather parallel to the plane. In the other dye molecules, there is little space because of more bulky axial ligands. Thus, these molecular structures are consistent with our observation of the different absorption spectra between SiPc2 and the others.

-----<<< Fig. 4 >>>-----

3.4. Device performance

-----<<< Fig. 5 >>>-----

Figure 5a shows the *J*–*V* characteristics of P3HT:PCBM:dye ternary blend solar cells and a P3HT:PCBM binary blend reference cell under AM1.5G simulated solar irradiation at an intensity of 100 mA cm^{-2}. Except for the device with SiPc2, all the other ternary blend solar cells exhibited improved device performance. Compared to the reference cell without dye, the short current density (J_{SC}) was almost the same at SiPc2, reached the maximum at SiPc4, and then slightly decreased at longer alkyl chain lengths (SiPc6 and SiPcB18). The open-circuit voltage (V_{OC}) was almost independent of the alkyl chain lengths although it slightly increased. The FF was almost the same at shorter alkyl chain length ($n \leq 4$) but clearly decreased at the longest chain (SiPcB18). Consequently, the power conversion efficiency (PCE) reached a maximum of 4.2% at SiPc4 and SiPc6, which is improved by 10% compared to the reference cell (3.8%). All the device parameters are summarized in Table 3.

-----<<< Table 3 >>>-----

To address the origin of the different device performances, we measured EQE spectra of P3HT:PCBM:dye ternary blend solar cells. For the devices with SiPc2, as shown in Fig. 5b, a broad EQE peak was observed at the P3HT absorption (400 – 600 nm), which was comparable to that of the reference cell without dye. However, no distinct EQE peak was observed at the dye absorption (680 nm), which was as low as ~10%. For the other devices, on the other hand, EQE peaks were observed both at the P3HT absorption (400 – 600 nm) and at the dye absorption (680 nm). The EQE peak at 400 – 600 nm slightly increased compared to that of the reference cell without dye, suggesting that P3HT excitons are effectively collected to dye molecules at the interface as reported previously.[18] The EQE peak at 680 nm was as high as ~50%.

4. Discussion

We start off our discussion by considering the energetics of P3HT:PCBM:dye ternary blend solar cells. As described above, the axial substituents have little impact on the electronic state in the phthalocyanine. Therefore, all the SiPc derivatives with different axial substituents exhibit almost the same HOMO (5.4 eV) and LUMO (3.5 eV) levels. The HOMO level of P3HT and the LUMO level of PCBM have been reported to be 4.8 eV[26] and 3.7 – 4.3 eV,[27,28] respectively. Therefore, the energy offset of the HOMO levels between P3HT and dye is as large as 0.6 eV and the energy offset of the LUMO levels between dye and PCBM is also as large as 0.2 – 0.8 eV. These offsets are large enough to induce the electron transfer between the LUMO levels of dye and PCBM and the hole transfer between the HOMO levels of dye and P3HT. In other words, these SiPc derivatives serve as an electron donor for PCBM and as an electron acceptor for P3HT. Indeed, we have recently reported rapid hole transfer (~2 ps) from SiPc6 to P3HT and prompt electron

transfer (<0.1 ps) from SiPc6 to PCBM upon the dye excitation.[18] We therefore conclude that the hole and electron transfers from dye excitons are energetically favorable for all the SiPc derivatives employed in this study.

Next, we consider the dye location in ternary blend films. Only the dye molecules located at the P3HT/PCBM interface can contribute to the photocurrent generation. As we reported previously, therefore, the internal quantum efficiency (IQE) can provide a good measure for estimating the fraction of dye molecules located at the interface. From the EQE and absorption efficiency mentioned before, the IQE is estimated to be as high as ~70% except for SiPc2. This is a lower limit because the charge transport efficiency is not always 100%, suggesting that most of the dye molecules are located at the interface. Indeed, a recent transient absorption study has demonstrated that almost all the SiPc6 molecules are located at the P3HT/PCBM interface.[18] For the device with SiPc2, the IQE is estimated to be as high as ~50% although it is lower than that for the other dyes, suggesting that the majority of SiPc2 molecules are located at the interface . We therefore conclude that the absence of improvement in J_{SC} of the P3HT:PCBM:SiPc2 solar cell is primarily due to the decrease in the absorption intensity and secondarily due to less interfacial segregation of SiPc2.

Finally, we focus on the device performance of ternary blend solar cells. As shown in Fig. 6, PCE of the ternary blend solar cells shows a maximum at around n = 4 and 6, suggesting that neither shorter nor longer axial chains are effective for the dye sensitization in ternary blend solar cells. This is because, as mentioned above, J_{SC} increases with increasing alkyl chains and then decreases slightly at longer chains while FF decreases at longer chains. In other words, it can be said that the maximum PCE results from the balance between J_{SC} and FF. As shown in P3HT:PCBM:SiPc2, dyes with shorter axial chains cause the aggregation and hence cannot contribute to the improvement in J_{SC}. On the other hand, as shown in P3HT:PCBM:SiPcB18, dyes with longer axial chains are hardly in close contact

with neighboring molecules and hence hinder efficient charge transfer or charge transport resulting in the decrease in FF. We therefore conclude that SiPc4 and SiPc6 are appropriate molecules as the light-harvesting dye in polymer solar cells because butyl or hexyl groups are large enough to suppress the dye aggregation and small enough to maintain close contact with neighboring molecules.

5. Conclusions

Five SiPc derivatives with different axial groups were synthesized to study how the axial groups have impact on the dye sensitization of P3HT:PCBM solar cells. Such different substituents have littile impact on the electronic state of phthalocyanine core unit or the interfacial distribution in P3HT:PCBM blend films. In contrast, the device parameters are substantially dependent on the subsituents: J_{SC} was almost the same at SiPc2, reached the maximum at SiPc4, and then slightly decreased at longer alkyl chain lengths (SiPc6 and SiPcB18) while FF was almost the same at shorter alkyl chain lengths ($n \leq 4$) but clearly decreased at the longest chain (SiPcB18). As a result, the devices with SiPc4 or SiPc6 show a maximum PCE of 4.2%, which is improved by 10% compared to that of the P3HT:PCBM control cell. Considering the molecular structure obtained by the DFT calculation, the axial size of SiPc4 or SiPc6 is comparable to the phthalocyanine conjugation plane. In other words, the butyl or hexyl chain is long enough to suppress dye aggregation and short enough to be in close contact with neighboring molecules. We therefore conclude that axial substituents should be modest in length to appropriately cover the conjugation plane of the phthalocyanine ring.

Acknowledgments

This work was partly supported by the FIRST program (Development of Organic

Photovoltaics toward a Low-Carbon Society: Pioneering Next Generation Solar Cell Technologies and Industries via Multi-manufacturer Cooperation), the JST PRESTO program (Photoenergy Conversion Systems and Materials for the Next Generation Solar Cells), and the Global COE program (International Center for Integrated Research and Advanced Education in Materials Science) from the Ministry of Education, Culture, Sports, Science, and Technology, Japan.

References

[1] C.J. Brabec, J.R. Durrant, MRS Bull. 33 (2008) 670.

[2] F.C. Krebs, Sol. Energy Mater. Sol. Cells 93 (2009) 394.

[3] M. Helgesen, R. Søndergaard, F.C. Krebs, J. Mater. Chem. 20 (2010) 36.

[4] G. Dennler, M.C. Scharber, C.J. Brabec, Adv. Mater. 21 (2009) 1323.

[5] C.J. Brabec, S. Gowrisanker, J.J.M. Halls, D. Laird, S. Jia, S.P. Williams, Adv. Mater. 22 (2010) 3839.

[6] W. Ma, C. Yang, X. Gong, K. Lee, A. J. Heeger, Adv. Funct. Mater. 15 (2005) 1617.

[7] G. Li, V. Shrotriya, J. Huang, Y. Yao, T. Moriarty, K. Emery, Y. Yang, Nat. Mater. 4 (2005) 864.

[8] Y. Kim, S. Cook, S.M. Tuladhar, S.A. Choulis, J. Nelson, J.R. Durrant, D.D.C. Bradley, M. Giles, I. McCulloch, C.-S. Ha, M. Ree, Nat. Mater. 5 (2006) 197.

[9] M.D. Irwin, D.B. Buchholz, A.W. Hains, R.P.H. Chang, T.J. Marks, Proc. Natl. Acad. Sci. USA 105 (2008) 2783.

[10] M.T. Dang, L. Hirsch, G. Wantz, Adv. Mater. 23 (2011) 3597.

[11] J. Peet, J.Y. Kim, N.E. Coates, W.L. Ma, D. Moses, A.J. Heeger, G.C. Bazan, Nat. Mater. 6 (2007) 497.

[12] E. Bundgaard, F.C. Krebs, Sol. Energy Mater. Sol. Cells 91 (2007) 954.

[13] R. Kroon, M. Lenes, J.C. Hummelen, P.W.M. Blom, B. de Boer, Polym. Rev. 48 (2008)

531.

[14] Y. Liang, L. Yu, Acc. Chem Res. 43 (2010) 1227.

[15] J. Peet, A.B. Tamayo, X.D. Dang, J.H. Seo, T.Q. Nguyen, Appl. Phys. Lett. 93 (2008) 163306.

[16] S. Honda, T. Nogami, H. Ohkita, H. Benten, S. Ito, ACS Appl. Mater. Interfaces 1 (2009) 804.

[17] S. Honda, H. Ohkita, H. Benten, S. Ito, Chem. Commun. 46 (2010) 6596.

[18] S. Honda, S. Yokoya, H. Ohkita, H. Benten, S. Ito, J. Phys. Chem. C 115 (2011) 11306.

[19] S. Honda, H. Ohkita, H. Benten, S. Ito, Adv. Energy Mater. 1 (2011) 588.

[20] A.D. Becke, J. Chem. Phys. 98 (1993) 1372.

[21] C. Lee, W. Yang, R.G. Parr, Phys. Rev. B 37 (1988) 785.

[22] K.E. Riley, B.T. Op`t Holt, K.M. Merz Jr, J. Chem. Theory Comput. 3 (2007) 407.

[23] J. Pommerehne, H. Vestweber, W. Guss, R.F. Mahrt, H. Bässler, M. Porsch, J. Daub, Adv. Mater. 7 (1995) 551.

[24] G. Cheng, X. Peng, G. Hao, V.O. Kennedy, I.N. Ivanov, K. Knappenberger, T.J. Hill, M.A.J. Rodgers, M.E. Kenney, J. Phys. Chem. A 107 (2003) 3503.

[25] Y. Liang, Z. Xu, J. Xia, S.-T. Tsai, Y. Wu, G. Li, C. Ray, L. Yu, Adv. Mater. 22 (2010) E135.

[26] I. McCulloch, C. Bailey, M. Giles, M. Heeney, I. Love, M. Shkunov, D. Sparrowe, S. Tierney, Chem. Mater. 17 (2005) 1381.

[27] C.J. Brabec, A. Cravino, D. Meissner, N.S. Sariciftci, T. Fromherz, M.T. Rispens, L. Sanchez, J.C. Hummelen, Adv. Funct. Mater. 11 (2001) 374.

[28] M.C. Scharber, D. Mühlbacher, M. Koppe, P. Denk, C. Waldauf, A.J. Heeger, C.J. Brabec, Adv. Mater. 18 (2006) 789.

Figure Captions

Fig. 1. Synthetic schemes of SiPc[OSi(C_nH_{2n+1})$_3$]$_2$ (SiPc*n*, *n* = 2, 3, 4, 6) and SiPc[OSi(iBu)$_2$$C_{18}H_{37}$]$_2$ (SiPcB18).

Fig. 2. Cyclic voltammograms of SiPc6 (solid line) and ferrocene (broken line) in dichlorobenzene/acetonitrile with TBAP. The scan rate is 100 mV s^{-1}.

Fig. 3. Absorption spectra of SiPc derivatives: SiPc2 (green lines), SiPc3 (orange lines), SiPc4 (red lines), SiPc6 (purple lines), and SiPcB18, (blue lines). a) the absorbance of the dyes in toluene solutions and b) the absorption efficiency of the dyes in P3HT:PCBM blend films that is estimated from twice the absorbance on the assumption that the incident light loss at the air/glass interface is 4% and the reflection at the metal electrode is 100%.[25] The broken line represent the absorption efficiency of P3HT:PCBM blend films without dye.

Fig. 4. Space-filling structures of SiPc2 (a) and SiPc3 (b) obtained by the DFT calculation.

Fig. 5. a) *J*–*V* characteristics of dye-sensitized polymer solar cells of P3HT:PCBM:dye ternary blends and the control cell of P3HT:PCBM binary blend under AM1.5G simulated solar illumination at 100 mW cm^{-2} in the air: SiPc2 (green lines), SiPc4 (red lines), SiPcB18, (blue lines), and without dye (broken lines). b) EQE spectra of the P3HT:PCBM:dye ternary blend and P3HT:PCBM binary blend solar cells.

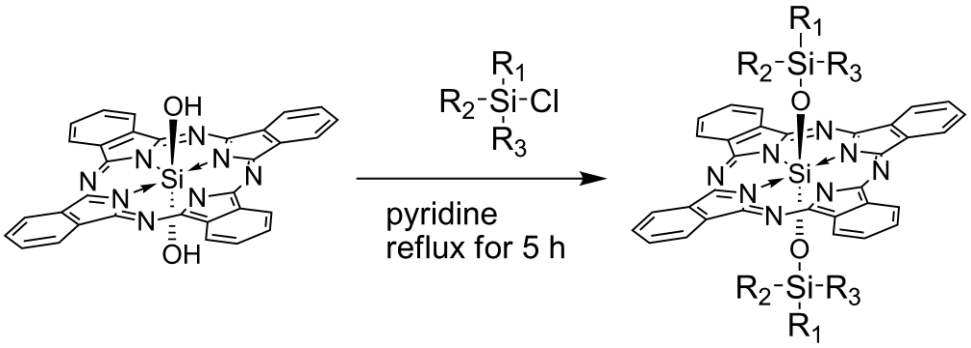
OH
Si
N
OH
R1
R2-Si-Cl
R3
pyridine
reflux for 5 h
R1
R2-Si-R3
O
Si
O
R2-Si-R3
R1

Fig. 1

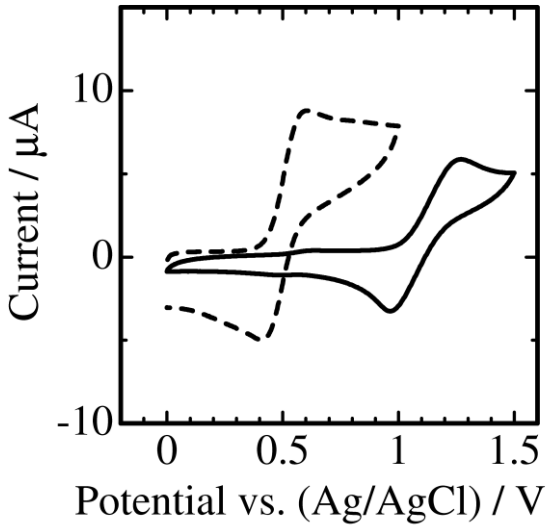

Fig. 2

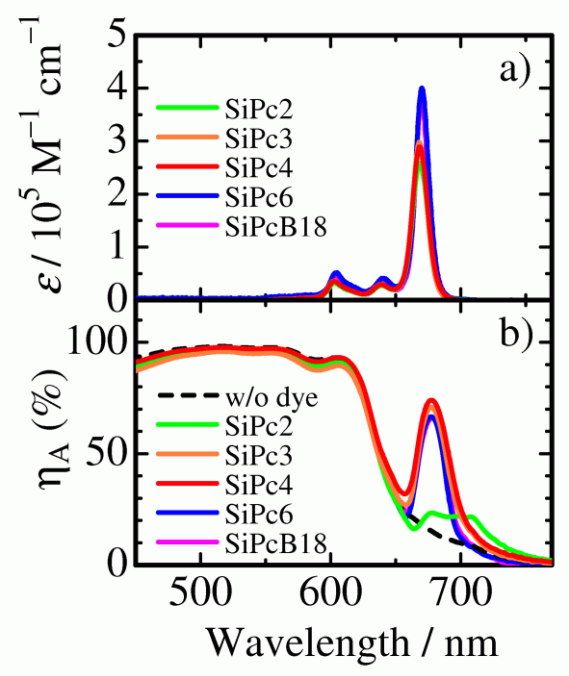
a)
b)
SiPc2
SiPc3
SiPc4
SiPc6
SiPcB18
w/o dye
ε / 10^5 M^-1 cm^-1
η_A (%)
Wavelength / nm
0
1
2
3
4
5
50
100
500
600
700

Fig. 3

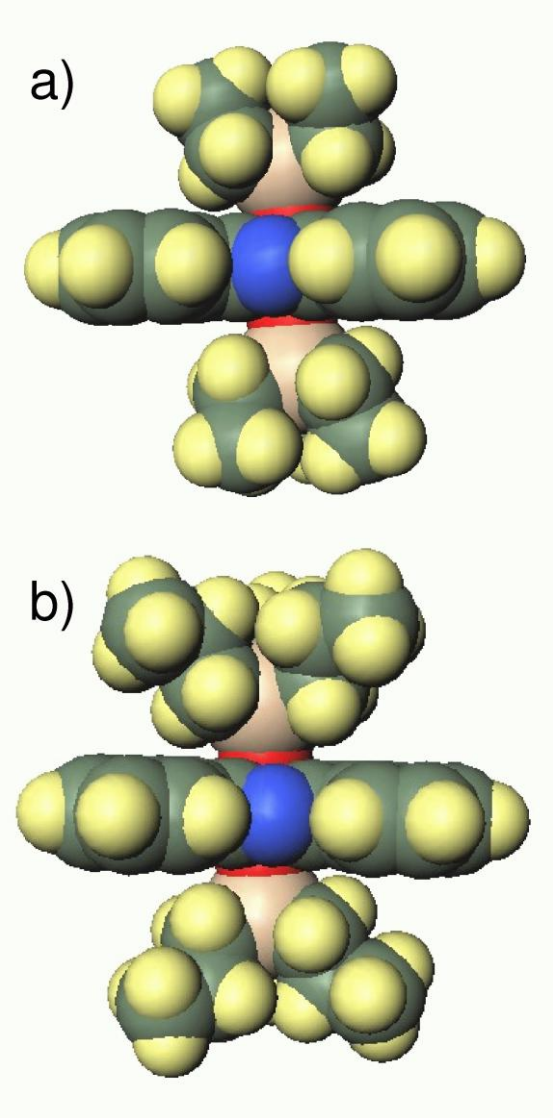

Fig .4

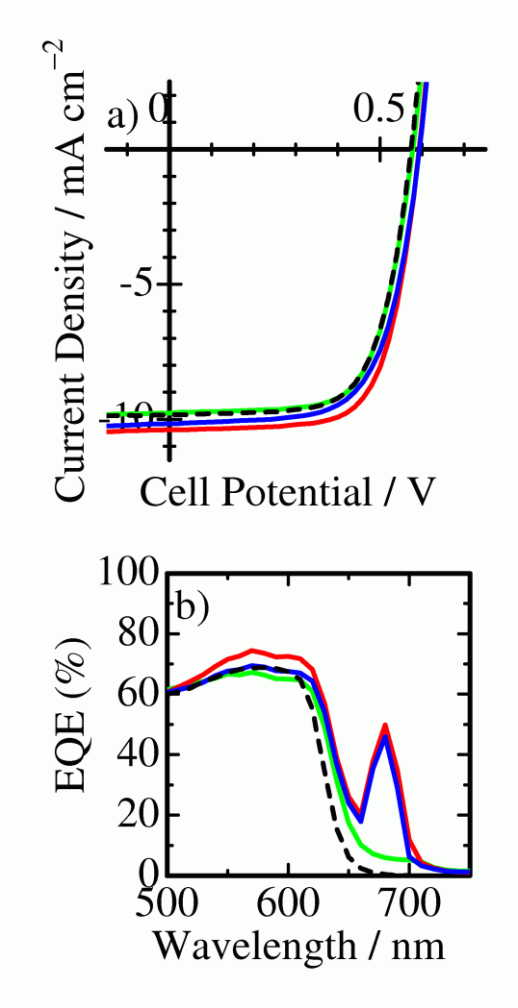
a)
0.5
-5
Current Density / mA cm^{-2}
Cell Potential / V
b)
100
80
60
40
20
0
EQE (%)
500
600
700
Wavelength / nm

Fig. 5